Hindawi
Active and Passive Electronic Components
Volume 2017, Article ID 3454165, 8 pages
https://doi.org/10.1155/2017/3454165

*Research Article*

# All-Pass Filter Based Linear Voltage Controlled Quadrature Oscillator

**Koushick Mathur,[1] Palaniandavar Venkateswaran,[2] and Rabindranath Nandi[2]**

[1]*Department of Electronics & Communication Engineering, UIT, Burdwan University, West Bengal 713104, India*
[2]*Department of Electronics & Telecommunication Engineering, Jadavpur University, Kolkata 700032, India*

Correspondence should be addressed to Rabindranath Nandi; robjutel@yahoo.co.in

Received 14 June 2017; Accepted 27 July 2017; Published 29 August 2017

Academic Editor: Jiun-Wei Horng



A linear voltage controlled quadrature oscillator implemented from a first-order electronically tunable all-pass filter (ETAF) is presented. The active element is commercially available current feedback amplifier (AD844) in conjunction with the relatively new Multiplication Mode Current Conveyor (MMCC) device. Electronic tunability is obtained by the control node voltage ($V$) of the MMCC. Effects of the device nonidealities, namely, the parasitic capacitors and the roll-off poles of the port-transfer ratios of the device, are shown to be negligible, even though the usable high-frequency ranges are constrained by these imperfections. Subsequently the filter is looped with an electronically tunable integrator (ETI) to implement the quadrature oscillator (QO). Experimental responses on the voltage tunable phase of the filter and the linear-tuning law of the quadrature oscillator up to 9.9 MHz at low THD are verified by simulation and hardware tests.

## 1. Introduction

Realization of first-order all-pass filters had been reported earlier using various types of active building blocks (ABBs), namely, VOA [1], Current Conveyor and its variants [2–5], DDA [6], DDCC [7], DVCC [8, 9], VDIBA [10], and OTA, with differential amplifier [11] as listed in Table 1; some of these building blocks are implemented with a basic device (OTA, CC, or DVCC) combined with some signal (current or voltage) differential unit. Recent literature suggests that electronic function circuits fabricated by commercially available IC modules are capable of providing desired results [12–16].

A varied genre of ABBs emerged during the recent past for realizing diverse functions towards signal processing/wave forming/filtering applications. Fabrication of internal design of such ABBs in CMOS technology leads to easy verification. However, recent studies address the issues of such approach concerning involvement of fabrication cost and complexity in their nodal relations with such wide variety of ABBs [12, 14, 16].

Use of readily available off-the-shelf devices thus may be an alternate approach to obtaining satisfactory results. Some recent composite blocks yield quite useful results on signal processing applications wherein two types of basic commercially available chips are conjoined (e.g., DDCC, DVCC, and VDIBA). It has been suggested that composite blocks may provide better results in comparison to the constituent elements [17]. So for such ABBs requiring more than one commercially available IC, it is still economical and more convenient compared to chip fabrication [12, 16, 17].

The relatively new MMCC element [18] used in this work is thus configured using readily available CFA (AD844) and multiplier (AD835) [19] elements. The useful feature of the MMCC is that it has an in-built control voltage terminal ($V$) which is conveniently utilized for electronic tuning of a circuit parameter. Hence the conventional method of transconductance ($g_m$) to bias current ($I_b$) conversion is avoided; such conversion needs additional hardware complexity and involvement of thermal voltage ($V_T$) [3, 10, 16]. We now present here an electronically tunable all-pass filter (ETAF) using the composite CFA-MMCC block.

Next a linear voltage controlled quadrature oscillator (LVCQO) is implemented with the ETAF being looped in feedback with an electronically tunable integrator (ETI).

Table 1: Comprehensive summary of recent APFs.

| Ref. | ABB | ABB implementation | $f_p$ reported (Hz) | Tunability |
|---|---|---|---|---|
| [1] | VOA | HA 2544C opamp | 125 K | $RC$ |
| [2] | CCII | LF 356N opamp with current mirror | 1.6 K | $RC$ |
| [3] | DO-CCCII | Dual-output current controlled conveyors | 1.63 M | $I_b$ |
| [4] | CCC II with OA | Current controlled conveyor | 12.15 K | $I_b$ |
| [5] | DO-CCII | CC II with additional z-copy node | 3.89 M | $RC$ |
| [6] | DDA | Differential amplifier (DA) | 16 K | $RC$ |
| [7] | DDCC | Current conveyor with DA | 318 K | $RC$ |
| [8] | DVCC | VDU followed by OTA | 400 K | $I_b$ |
| [9] | DVCC | VDU followed by CC | 1.59 M | $RC$ |
| [10] | VDIBA | OTA with differential input buffer | 9.4 M | $I_b$ |
| [11] | OTA | OTA with DA | 375 K | $I_b$ |
| Proposed | CFA-MMCC | CFA844 and multiplier AD835 | 9.91 M | $V$ |

*Notes.* (a) Designs in [1, 2, 10], based on commercially available IC modules; (b) comprehensive listing of recent APFs using various ABBs presented in [5].

Detailed analysis is carried out taking into account the device imperfections, namely, parasitic shunt-$r_zC_z$ components and the roll-off poles of the port-transfer ratios. Effects of these nonidealities are negligible but the higher range of usable frequencies is constrained. The oscillation frequency ($\omega_o$) is active-insensitive relative to port-mismatch error ($\varepsilon$). Experimental results on ETAF and quadrature oscillator responses are verified by PSPICE simulation and hardware test.

## 2. Analysis

The proposed ETAF is shown in Figure 1(a) where the nodal relations are as follows:

$$\text{CFA: } I_z = \alpha I_x,\ V_x = \beta V_y, \text{ and } V_o = \delta V_z$$
$$\text{MMCC: } I_z = aI_x,\ V_x = b(kV_{y1}V_{y2}), \text{ and } V_w = \gamma V_z.$$

The port tracking ratios are ideally unity but may be postulated by error coefficients ($|\varepsilon| \ll 1$) as $\alpha = (1 - \varepsilon_i) = a$, $\beta = (1 - \varepsilon_v) = b$, and $\delta = (1 - \varepsilon_z) = \gamma$, where $k \equiv (0.1/\text{volt})$ is the multiplication constant [20].

Analysis of Figure 1(a) yields the transfer function $G \equiv V_o/V_i$ as

$$G = \frac{\{\delta_1\delta_2 m + (\delta_1\delta_2 - 1)\alpha_2\beta_2\}\, sn\tau - \{\alpha_1\alpha_2\delta_1\delta_2 ab\gamma\}}{[sn\tau + \alpha_1\delta_1 ab\gamma]} \quad (1)$$

parasitic elements, yielding a modified transfer where $m = r_3/r_4$, $n = r_2/r_1$, and $\tau = RC/kV$.

In ideal devices port tracking ratios are all unity; assuming the realizability conditions as $m = 1 = n$ ($r_{1,2,3,4} = r$) for simplicity, we get

$$G = \frac{(s\tau - 1)}{(s\tau + 1)} \quad (2)$$

which is the nonminimum phase all-pass function, where transmission gain $|G| = 1$ and phase ($\theta$) is tunable in a range $180 \le \theta^\circ \le 0$, being variable by control voltage ($V$) as

$$\theta = \pi - 2\arctan\left(\frac{\omega RC}{kV}\right). \quad (3)$$

## 3. Effects of Nonidealities

*3.1. Parasitic Components.* The parasitic components appear as shunt-$r_zC_z$ arms at current source nodes of the device; as per data-book [21], the typical values are $2 \le r_z\,(\text{M}\Omega) \le 5$ and $3 \le C_z\,(\text{pF}) \le 5.5$; ratio of circuit resistors (K$\Omega$) relative to $r_z$ is assumed to be negligible. Reanalysis now with finite parasitic elements yields modified transfer elements in Figure 1(a) exhibiting a single-pole roll-off model [22], given by

$$\widehat{G} = \frac{\left(n_2 s^2 + n_1 s + n_o - 1\right)}{\left(d_3 s^3 + d_2 s^2 + d_1 s + d_o + 1\right)}, \quad (4)$$

where

$$n_2 = \tau\tau_{z1}(1 + \sigma)$$
$$n_1 = \tau(1 + \sigma)(1 + \mu_1) + (\mu_3\tau_{z1})$$
$$n_o = \mu_3(1 + \mu_1)$$
$$d_3 = \tau\tau_{z1}\tau_{z2}(1 + \sigma)$$
$$d_2 = \{\tau\tau_{z1}(1 + \sigma)(1 + \mu_2)\} + \tau\tau_{z2}\{(1 + \sigma)(1 + \mu_1)\} + (\mu_3\tau_{z1}\tau_{z2})$$
$$d_1 = \tau\{(1 + \sigma)(1 + \mu_1) + (\mu_3\tau_{z1})\}(1 + \mu_2) + \{\tau_{z2}\mu_3(1 + \mu_1)\}$$
$$d_o = \mu_2$$
$$\sigma = \frac{C_{z3}}{C} \ll 1,$$
$$\mu_{1,2} = \frac{r}{r_{z1,2}} \ll 1,$$

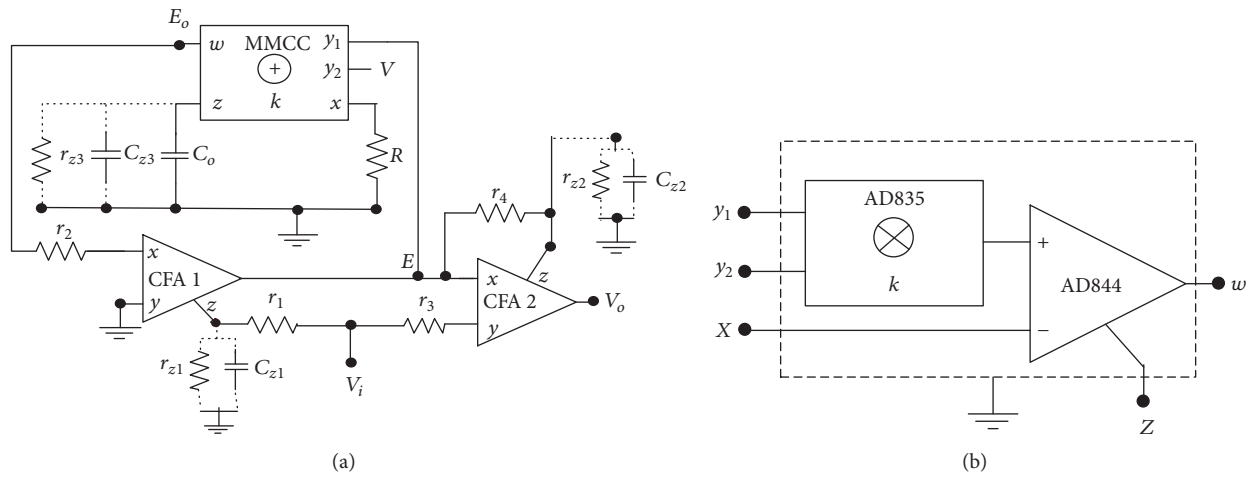


Figure 1: (a) First-order ETAF. (b) Implementation of MMCC with commercially available ICs.

$$\mu_3 = \frac{R}{kVr_{z3}} \ll 1$$

$$\tau_{z1,2} = rC_{z1,2},$$

$$\frac{\tau_{z1,2}}{\tau} \ll 1. \tag{5}$$

Then (4) simplifies to

$$\widehat{G} = \frac{\left[s^2\tau\tau_{z1} + s\tau - 1\right]}{\left[s^3\tau\tau_{z1}\tau_{z2} + s^2\left(\tau_{z1} + \tau_{z2}\right) + s\tau + 1\right]}. \tag{6}$$

The frequency-domain behavior may be estimated by writing $s = j\omega$ in (6), given by

$$\widehat{G}(\omega) = \frac{\left[j\omega\tau - \left(1 + \zeta_1\right)\right]}{\left[j\left\{\omega\tau\left(1 - \zeta_2\right)\right\} + \left(1 - \zeta_3\right)\right]}, \tag{7}$$

where

$$\zeta_1 = \frac{\omega^2}{\omega_p\omega_{z1}} \ll 1;$$

$$\omega_p\,(\text{filter-pole frequency}) = \frac{1}{\tau},\ \omega_{z1} = \frac{1}{\tau_{z1}};$$

$$\zeta_2 = \frac{\omega^2}{\omega_{z2}\omega_{z1}} \ll 1 \tag{8}$$

$$\zeta_3 = \omega^2\tau\left(\tau_{z1} + \tau_{z2}\right)\Big|_{\tau z1=\tau z2=\tau z} \approx 2\omega^2\tau\tau_z \approx \frac{2\omega^2}{\omega_p\omega_z} \ll 1.$$

With $C_z \approx 3.3$ pF (measured) and $r = 1$ KΩ, we estimated value of the parasitic pole frequency $f_z \approx 54$ MHz. Hence for usable ranges of $< f_z$, effects of parasitic capacitors are negligible and $\widehat{G} = G$; therefore the nominal APF function is preserved with the limit $f \le f_z$.

*3.2. Roll-Off Pole of Device-Port Transfer Ratios.* At relatively high-frequency ranges, the port-transfer ratios $\alpha$, $\beta$, $\delta$ and $a$, $b$, $\gamma$ of the active components are as follows:

$$\alpha_{1,2} = \frac{\alpha_{o1,2}}{\left(sp_{1,2} + 1\right)}$$

$$\delta_{1,2} = \frac{\delta_{o1,2}}{\left(sp_{3,4} + 1\right)}$$

$$\beta_2 = \frac{\beta_{o2}}{\left(sp_5 + 1\right)}$$

$$a = \frac{a_o}{\left(sp_i + 1\right)} \tag{9}$$

$$b = \frac{b_o}{\left(sp_v + 1\right)}$$

$$\gamma = \frac{\gamma_o}{\left(sp_z + 1\right)}.$$

The dc values of all the products of port coefficients in (1) may be taken as unity; for example, $\alpha_{o1,2} \approx \{1 - (\varepsilon_{i1} + \varepsilon_{i2})\} \approx 1$ since $\varepsilon_{i1,2} \ll 1$.

The modified APF function ($G'$) is now written as

$$G' = \frac{\left[\Delta_1 + \Delta_2\left(\Delta_1 - 1\right)s\tau - \Delta_3 M\right]}{\left[s\tau + \Delta_4 M(s)\right]}, \tag{10}$$

where

$$\Delta_1 = \delta_1\delta_2 \approx \frac{1}{\left\{s^2 p_3 p_4 + s\left(p_3 + p_4\right) + 1\right\}} \tag{11}$$

$$\Delta_2 = \alpha_2\beta_2 \approx \frac{1}{\left\{s^2 p_1 p_5 + s\left(p_1 + p_5\right) + 1\right\}} \tag{12}$$

$$\Delta_3 = \alpha_1\alpha_2 \approx \frac{1}{\left\{s^2 p_1 p_2 + s\left(p_1 + p_2\right) + 1\right\}} \tag{13}$$

$$\Delta_4 = \alpha_1\delta_1 \approx \frac{1}{\left\{s^2 p_1 p_3 + s\left(p_1 + p_3\right) + 1\right\}}. \tag{14}$$

Table 2: Comparative description of recent QO designs.

| Ref. | Device used | Electronic tunability | Linear tuning law | $f_o$ reported (Hz) | Tuning by | THD (%) |
|---|---|---|---|---|---|---|
| [5] | DO-CCII | No | No | 2.33 M | $RC$ | 1.17~2.82 |
| [10] | VDIBA | Yes | No | 8.5 M | $\sqrt{I_b}$ | 2.25 |
| [12] | CFA | No | No | 909 K | $RC$ | — |
| [14] | CFA | No | No | 398 K | $RC$ | 1.42 |
| [23] | OTA | Yes | Yes | 64 K | $I_b$ | — |
| [24] | VOA | No | No | 160 K | $RC$ | — |
| [25] | CFOA | No | No | 159 K | $RC$ | 3.16 |
| [26] | CDTA | Yes | No | 1.73 M | $\sqrt{I_b}$ | 3.0 |
| [27] | CCCDBA | Yes | No | 419 K | $\sqrt{I_b}$ | 2~1.2 |
| [28] | CCCCTA | Yes | No | 1.1 M | $\sqrt{g_m}$ | 1~2.9 |
| [29] | OTA | Yes | No | 1.59 M | $\sqrt{g_m}$ | 1~2.2 |
| Proposed | CFA-MMCC | Yes | Yes | ~10.2 M | $V$ | 0.9 ~2.8 |

The function $M(s)$ relates to the MMCC block; it is decomposed as $M(s) = M_o(s) \cdot M_e(s)$, where $M_o = 1/s\tau_o$ and

$$M_e(s) = \frac{1}{[(sp_i + 1)(sp_v + 1)(sp_z + 1)]}. \quad (15)$$

It has been observed that the 3 dB corner frequencies for all the port-transfer ratios appear at close proximity, and hence these may be assumed equal without loss of generality [22]. Therefore calculations for examining the effects of the roll-off poles become simpler if we write $p_{1\sim5} \equiv 1/\omega_p$. Writing $u = (\omega/\omega_p) \ll 1$ and solving for (11) we get

$$\Delta_1(j\omega) = \frac{1}{\{1 - u^2 + 2ju\}} \quad (16)$$

which implies $|\Delta_1| = \sqrt{(1+4u^2)} \approx 1$ and $\angle\Delta_1 = \arctan(2u) \approx 0$. Similar results are checked for (12) to (14). For the effects of the MMCC roll-off, we put $\psi = (\omega/\omega_m) \ll 1$, where $p_{i,v,z} \equiv 1/\omega_m$; solving (15), we get

$$M_e(j\omega) = \frac{1}{[(1 - 3\psi^2) + j3\psi\{1 - (\psi^2/3)\}]} \quad (17)$$

which reduces to $|M_e| = 1$ and $\angle M_e = -\arctan(3\psi) \approx 0$. This analysis indicates that effects of roll-off poles of the active building blocks are quite negligible in the range of operating frequencies ($f < f_{p,m}$).

## 4. LVCQO Implementation

Quadrature oscillators find diverse application in measurement systems [30–33] and in communication circuits, quadrature mixers, SSB-modulator, vector generator, and data conversion. A comprehensive summary of recent QO designs is listed in Table 2. It may be seen that even though a number of such oscillators were reported, very few are linearly tunable.

We now present the linear VCO as implemented by forming a regenerative feedback loop formed with the ETAF in Figure 1(a) and the ETI in Figure 2; transfer of ETI is

$$H(s) = \frac{1}{\{s\tau_o(1 + \xi) + (R_o/r_z)\}}, \quad (18)$$

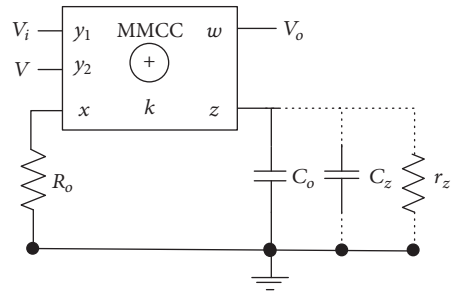


Figure 2: Electronically tunable integrator (ETI).

where $\tau_o = R_oC_o/kV$, $\xi = C_o/C_z \ll 1$, and $R_o/r_z \ll 1$; hence $H(s) = 1/s\tau_o$. Grounding of the capacitor ($C$) facilitates absorbing $C_z$ in $C$-values at predesign level. Device imperfection relative to port-transfer roll-off pole frequencies ($\omega_{a,b,\gamma}$) is estimated by writing

$$H(s) = \frac{(ab\gamma)}{s\tau_o} \equiv \frac{(1 - \varepsilon_T)}{\{(s\tau_o)\,\text{H}\}}, \quad (19)$$

where $\varepsilon_T = (\varepsilon_i + \varepsilon_v + \varepsilon_z) \ll 1$.

The deviation due to roll-off is

$$\text{H} = \left\{\left(\frac{s}{\omega_a}\right) + 1\right\}\left\{\left(\frac{s}{\omega_b}\right) + 1\right\}\left\{\left(\frac{s}{\omega_\gamma}\right) + 1\right\}. \quad (20)$$

As in previous section if we assume $\omega_{a,b,\gamma} \approx \omega_m$ and put $\psi = (\omega/\omega_m)$, then H reduces similar to (17) as

$$|\text{H}| = 1,$$
$$\angle\text{H} = -\arctan(3\psi) \approx 0. \quad (21)$$

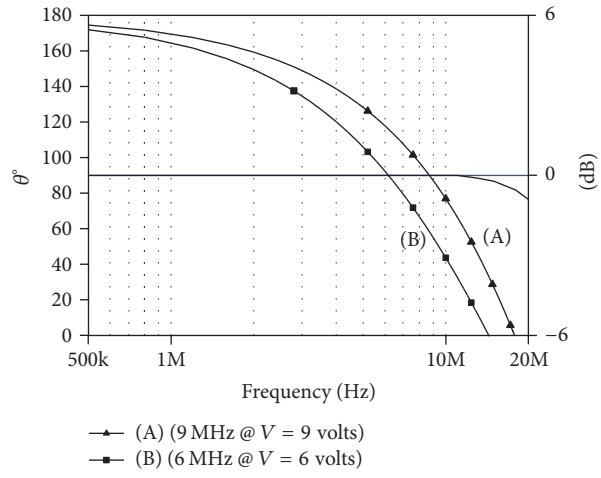


| $\theta_e$ \| $f_p$ (MHz) |
|---|
| (A) 3.1° at $f_p$ = 9.0 |
| (B) 1.2° at $f_p$ = 6.0 |

(a)

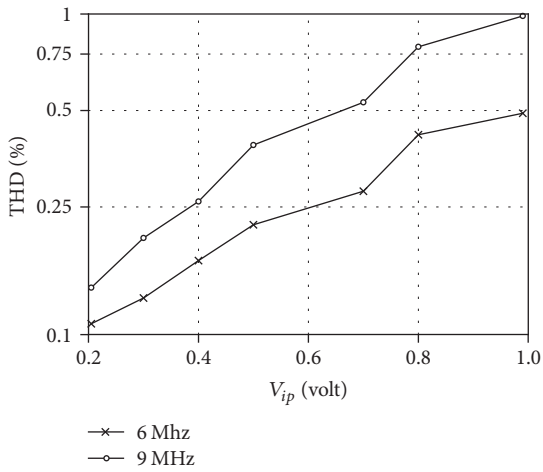


(b)

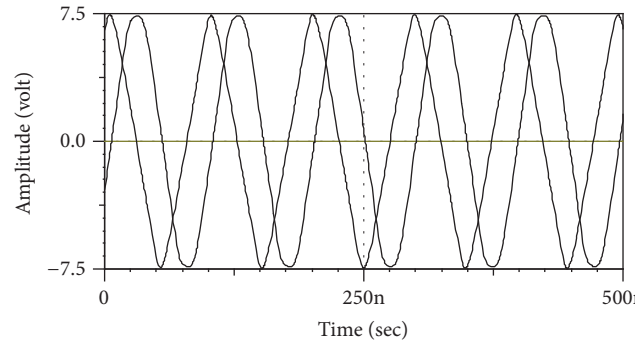


(c)

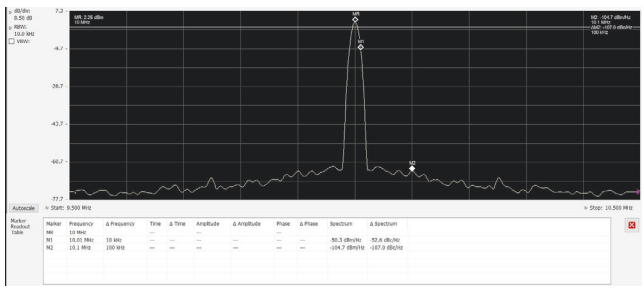

(d)

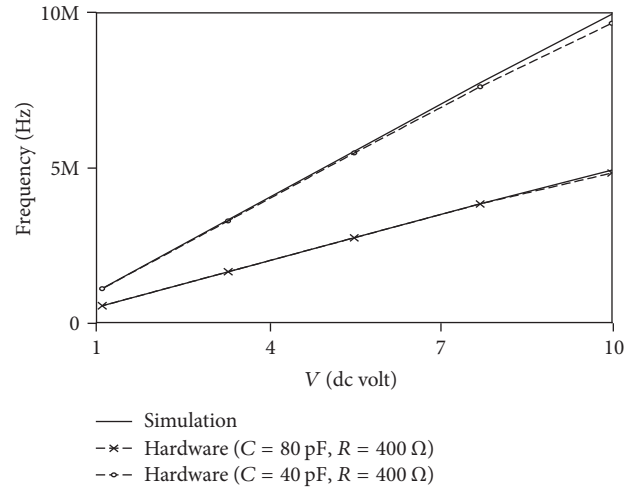


(e)

Figure 3: Continued.

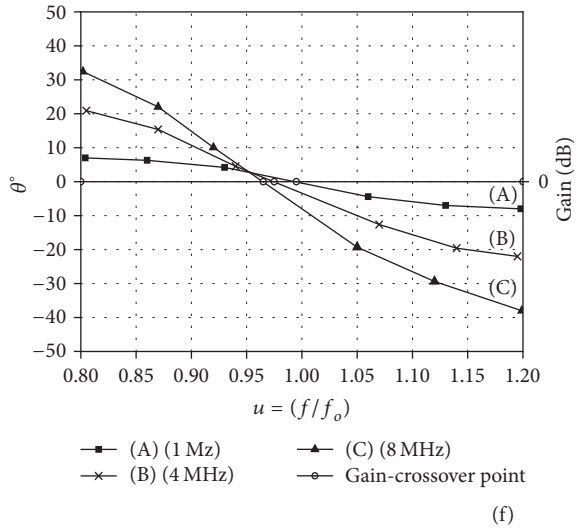


(f)

| $f_o$ (MHz) | Quadrature phase error ($\Delta\theta$) | THD% |
|---|---|---|
| 2 | 1.2° | 0.6 |
| 6 | 2.4° | 1.6 |
| 10 | 3.1° | 2.8 |

FIGURE 3: Measured response of ETAF and QO. (a) AP phase response: (A) = 9 V.d.c.; (B) = 6 V.d.c. (b) AP-THD (%) to 7th harmonic. (c) QO wave response tuned at 10 MHz quadrature signals at $V_o$ and $E_o$ nodes. (d) QO spectral response of 10 MHz for phase-noise evaluation. (e) QO linear-tuning response. (f) Measured tuning error of VCO.

Now implementation of oscillator is derived by equating $\{1 - GH(s)\} \equiv 0$ which gives the characteristic equation (CE):

$$\begin{aligned} \text{CE:} \quad & s^2\tau_o\tau + s(\tau_o - \tau) + 1 = 0 \\ \text{Realizability condition:} \quad & \tau_o = \tau \\ & R = R_o, \\ & C = C_o \\ \text{Oscillation frequency:} \quad & \omega_o = \frac{kV}{RC}. \end{aligned} \tag{22}$$

So tuned frequency ($f_o$ in Hz) is linearly and directly variable by control voltage ($V$)

$$f_o = \frac{V}{(20\pi RC)}. \tag{23}$$

The proposed method provides direct electronic tunability of oscillation frequency by the control voltage ($V$). No additional current processing circuitry for $g_m$ to bias current ($I_b$) conversion is needed, as seen in the previous designs shown in Table 1, and thermal voltage ($V_T$) is not involved. It may be seen that $\omega_o$ is practically active-insensitive, $S_\varepsilon^{\omega o} \approx 0.5\varepsilon \ll 1$.

## 5. Experimental Results

The response of $V$-tunability of the proposed ETAF and LVCQO had been verified by PSPICE simulation [34] and hardware tests; these are shown in Figure 3. ETAF responses, along with its phase error ($\theta_e$) and THD (measured to 7th harmonic), are shown in Figures 3(a) and 3(b) which are relatively low compared to [10, 24, 25]. Some small phase error ($\theta_e$) on the experimentally generated sinusoid quadrature signals deviated around 90° was measured as shown in Figure 3(c). The oscillator spectral response in Figure 3(d) shows the LVCQO spectral response wherein phase noise measured is −107 dBc/Hz at an offset of 100 KHz from the tuned frequency of 10 MHz; this response is measured by Tektronix spectrum analyzer (RSA306B) [35].

This result is better as compared to that in [14]. A new method of examining the VCO tuning error ($\beta$%) is adopted by measuring the shift ($\Delta f$) in $f_o$ at phase cross-over frequency. The tested value of $\beta$% in the overall tuning range of 1 MHz~10 MHz was observed to be less than 4.5%.

## 6. Conclusion

A new design of ETAF function and its subsequent application to the implementation of a VCQO with linear-tuning law are presented. The active blocks are commercially available CFA (AD844) and four-quadrant multiplier (AD835) which are readily available IC modules. Responses of the function circuits are verified experimentally with PSPICE simulation and hardware tests. The quadrature oscillator had been tuned by control voltage ($V$) in a linear range (band-spread) of $0.5 \leq f_o\,(\text{MHZ}) \leq 9.9$ at low THD. The design does not need any additional current processing circuitry; hence there is no extra quiescent dissipation. Power dissipation of the proposed oscillator circuit is about 33 mW. The circuit is practically active-insensitive relative to device-port track-error ($\varepsilon$). Analysis on the effects of device parasitic components indicates insignificant effect on design equations, even though parasitic capacitors tend to limit the usable high-frequency range. In this work, a relatively new building block, namely, the MMCC, had been utilized for the voltage ($V$) controlled linearly tunable quadrature oscilator design with 107 dBc/Hz phase noise at 100 KHz offset as shown in Figure 3(d). Thus a comparatively better quality result had been obtained as is shown in Table 2.

It may be seen in Tables 1 and 2 that in the cited designs active devices used are certain primary blocks with auxiliary voltage/current differencing unit (VDU/CDU) or differential amplifiers with their associated parasitics which tend to limit the desired range of frequency ($f_p$ or $f_o$) [6]. Also, tuning by $g_m$ or $I_b$ needs additional current processing circuits with parasitic capacitors. The authors believe that, owing to such topological distinction, the frequency tuning ranges are somewhat lower. However in the case of design by VDIBA [10], the range improves owing to the fact that the active component OPA-860 has itself a bandwidth (BW) of 470 MHz. In the proposed design, no such VDU/CDU and $g_m$-to-$I_b$ conversion circuitry are used; this circuit is structured with commercially available AD844 (BW = 60 MHz) and AD835 (250 MHz) IC modules to achieve relatively higher frequency, wherein effects of port-mismatch roll-off poles and parasitics had been included in support.

## Conflicts of Interest

The authors declare that they have no conflicts of interest.

## References


[1] S. J. G. Gift, "Application of all-pass filters in the design of multiphase sinusoidal systems," *Microelectronics Journal*, vol. 31, no. 1, pp. 9–13, 2000.

[2] M. Higashimura and Y. Fukui, "Realization of current mode all-pass networks using a current conveyor," *IEEE Transactions on Circuits and Systems*, vol. 37, no. 5, pp. 660-661, 1990.

[3] S. Öztayfun, S. Kilinç, A. Çelebi, and U. Çam, "A new electronically tunable phase shifter employing current-controlled current conveyors," *International Journal of Electronics and Communications*, vol. 62, no. 3, pp. 228–231, 2008.

[4] S. Minaei and O. Cicekoglu, "A Resistorless realization of the first-order all-pass filter," *International Journal of Electronics*, vol. 93, no. 3, pp. 177–183, 2006.

[5] F. Yucel and E. Yuce, "CCII based more tunable voltage-mode all-pass filters and their quadrature oscillator applications," *International Journal of Electronics and Communications*, vol. 68, no. 1, pp. 1–9, 2014.

[6] A. Toker and S. Özoğuz, "Novel all-pass filter section using differential difference amplifier," *International Journal of Electronics and Communications*, vol. 58, no. 2, pp. 153–155, 2004.

[7] J.-W. Horng, C.-M. Wu, and N. Herencsar, "Fully differential first-order allpass filters using a DDCC," *Indian Journal of Engineering and Materials Sciences*, vol. 21, no. 4, pp. 345–350, 2014.

[8] T. Tsukutani, H. Tsunetsugu, Y. Sumi, and N. Yabuki, "Electronically tunable first-order all-pass circuit employing DVCC and OTA," *International Journal of Electronics*, vol. 97, no. 3, pp. 285–293, 2010.

[9] M. A. Ibrahim, S. Minaei, and E. Yuce, "All-pass sections with rich cascadability and IC realization suitability," *International Journal of Circuit Theory and Applications*, vol. 40, no. 5, pp. 461–472, 2012.

[10] N. Herencsar, S. Minaei, J. Koton, E. Yuce, and K. Vrba, "New resistorless and electronically tunable realization of dual-output VM all-pass filter using VDIBA," *Analog Integrated Circuits and Signal Processing*, vol. 74, no. 1, pp. 141–154, 2013.

[11] A. Ü. Keskin, K. Pal, and E. Hancioglu, "Resistorless first-order all-pass filter with electronic tuning," *International Journal of Electronics and Communications*, vol. 62, no. 4, pp. 304–306, 2008.

[12] S. Maheshwari and M. S. Ansari, "Catalog of realizations for dxccii using commercially available ics and applications," *Radioengineering*, vol. 21, no. 1, pp. 281–289, 2012.

[13] S. J. G. Gift and B. Maundy, "An improved multiphase sinusoidal oscillator using current feedback amplifier," *International Journal of Electronics*, vol. 4, pp. 177–187, 2016.

[14] H.-P. Chen, Y.-S. Hwang, Y.-T. Ku, S.-F. Wang, and C.-H. Wu, "Voltage-mode universal biquadratic filter and quadrature oscillator using CFAs," *IEICE Electronics Express*, vol. 13, no. 15, pp. 1–11, 2016.

[15] R. Sotner, J. Jerabek, N. Herencsar, J.-W. Horng, K. Vrba, and T. Dostal, "Simple oscillator with enlarged tunability range based on ECCII and VGA utilizing commercially available analog multiplier," *Measurement Science Review*, vol. 16, no. 2, pp. 35–41, 2016.

[16] S. Siripongdee and W. Jaikla, "Electronically controllable grounded inductance simulators using single commercially available IC: LT1228," *International Journal of Electronics and Communications*, vol. 76, pp. 1–10, 2017.

[17] S. J. G. Gift and B. Maundy, "Versatile composite amplifier configuration," *International Journal of Electronics*, vol. 102, no. 6, pp. 993–1006, 2014.

[18] Y.-S. Hwang, W.-H. Liu, S.-H. Tu, and J.-J. Chen, "New building block: multiplication-mode current conveyor," *IET Circuits, Devices and Systems*, vol. 3, no. 1, pp. 41–48, 2009.

[19] "Analog Devices AD-835: 250 MHz, voltage output four quadrant multiplier," http://www.analog.com/datasheets/AD835.pdf.

[20] "Intersil datasheet file # 2477.5, Sept 1998; 2863.4 Apr. 1999".

[21] "Analog devices, Linear products data-book, (MA, USA)," 1990.

[22] E. Yuce and S. Minaei, "A modified CFOA and its applications to simulated inductors, capacitance multipliers, and analog filters," *IEEE Transactions on Circuits and Systems*, vol. 55, no. 1, pp. 266–275, 2008.

[23] K. Kumwachara and W. Surakampontorn, "An integrable temperature-insensitive gm-RC quadrature oscillator," *International Journal of Electronics*, vol. 90, no. 9, pp. 599–605, 2003.

[24] J.-W. Horng, "Quadrature oscillators using operational amplifiers," *Active and Passive Electronic Component*, vol. 2011, Article ID 320367, 4 pages, 2011.

[25] A. Lahiri, W. Jaikla, and M. Siripruchyanun, "First CFOA-based explicit-current-output quadrature sinusoidal oscillators using grounded capacitors," *International Journal of Electronics*, vol. 100, no. 2, pp. 259–273, 2013.

[26] J. Jin and C. Wang, "Single CDTA-based current-mode quadrature oscillator," *International Journal of Electronics and Communications*, vol. 66, no. 11, pp. 933–936, 2012.

[27] F. Khateb, W. Jaikla, D. Kubánek, and N. Khatib, "Electronically tunable voltage-mode quadrature oscillator based on high performance CCCDBA," *Analog Integrated Circuits and Signal Processing*, vol. 74, no. 3, pp. 499–505, 2013.

[28] W. Sa-Ngiamvibool and A. Jantakun, "Quadrature oscillator using CCCCTAs and grounded capacitors with amplitude controllability," *International Journal of Electronics*, vol. 101, no. 12, pp. 1737–1758, 2014.

[29] N. Pandey and R. Pandey, "Approach for third order quadrature oscillator realisation," *IET Circuits, Devices and Systems*, vol. 9, no. 3, pp. 161–171, 2015.

[30] J. Raman, P. Rombouts, and L. Weyten, "Simple quadrature oscillator for BIST," *Electronics Letters*, vol. 46, no. 4, pp. 271–273, 2010.

[31] D. Chen, W. Yang, and M. Pan, "Design of impedance measuring circuits based on phase-sensitive demodulation technique," *IEEE Transactions on Instrumentation and Measurement*, vol. 60, no. 4, pp. 1276–1282, 2011.

[32] S. Yoder, M. Ismail, and W. Khalil, *VCO-Based Quantizers Using Frequency-to-Digital and Time-to-Digital Converters*, SpringerBriefs in Electrical and Computer Engineering, Springer Sc. + Busines Media, LLC, New York, NY, USA, 2011.

[33] S. Liang and W. Redman-White, "A linear tuning ring VCO for spectrum monitor receiver in cognitive radio applications," in *Proceedings of the 20th European Conference on Circuit Theory and Design (ECCTD '11)*, pp. 65–68, IEEE, Linkoping, Sweden, August 2011.

[34] "Macromodel of AD-844 AN in PSPICE Library Microsim Corp., Irvine, USA," 1992.

[35] http://www.tek.com/spectrum-analyzer/rsa306.